GROUPS OF ENCASED STONE COLUMNS: INFLUENCE OF COLUMN LENGTH AND ARRANGEMENT

by

Jorge Castro

Group of Geotechnical Engineering

Department of Ground Engineering and Materials Science

University of Cantabria

Avda. de Los Castros, s/n

39005 Santander, Spain

Tel.: +34 942 201813

Fax: +34 942 201821

e-mail: castrogj@unican.es

Date: November 2016

Number of words: 6,000

Number of tables: 9

Number of figures: 17

ABSTRACT

This paper presents a set of systematic 2D and 3D finite element analyses that study the performance of groups of encased stone columns beneath a rigid footing. Those numerical analyses show that, if the area replacement ratio, i.e. area of the columns over area of the footing, and the ratio of encasement stiffness to column diameter are kept constant, the column arrangement (both number of columns and column position) has a small influence on the settlement reduction achieved with the treatment. For high encasement stiffnesses, placing the column near the footing edges may be slightly more beneficial reducing the settlement; on the contrary, the maximum hoop force at the encasement is notably higher. Based on the minor influence of column arrangement, this paper proposes a new simplified approach to study groups of encased stone columns, which involves converting all the columns of the group beneath the footing in just one central column with an equivalent area and encasement stiffness. This simplified model is used to conclude that, for settlement reduction and fully encased columns in a homogeneous soil, there is a column critical length of around two or three times the footing width. The critical length of the encasement for partially encased columns is slightly lower than that of the fully encased columns.

KEYWORDS: Geosynthetics, encased stone columns, numerical analyses, settlement, footings, critical length.

NOTATION

a_r	Area replacement ratio: $a_r = A_c / A_l$
c	Cohesion
c_u	Undrained shear strength
d_c	Column diameter
K_0	Coefficient of lateral earth pressure at rest
p_a	Uniform applied vertical pressure
p'_0	Initial mean effective stress
r	Radius
s	Centre-to-centre column spacing
s_x, s_y	Horizontal displacement
s_z	Settlement
s_{z0}	Settlement without columns
x,y,z	Cartesian coordinates
A	Cross-sectional area
B	Footing width
E	Young's modulus
E_{oed}	Oedometric (confined) modulus
F_g	Tensile hoop force at the encasement
H	Soft soil layer thickness
J_g	Encasement stiffness
L	Length
N	Number of columns in the group

β	Settlement reduction factor: $\beta = s_z / s_{z0}$
γ'	Effective unit weight
ε	Strain
ν	Poisson's ratio
σ	Stress
ϕ	Friction angle
ψ	Dilatancy angle

Subscripts:

c,s,g,l	column, soil, encasement, loaded area
x,y,z	Cartesian coordinates

1. INTRODUCTION

Ground improvement using stone columns is a popular technique for foundation of embankments or structures on soft soils. Stone columns are vertical boreholes in the ground, filled upwards with gravel compacted by means of a vibrator. The inclusion of gravel, which has a higher strength, stiffness and permeability than the natural soft soil, improves the bearing capacity of the soft foundation thus enhancing stability of the embankments, reduces total and differential settlements, accelerates soil consolidation and reduces the liquefaction potential (e.g. Barksdale and Bachus, 1983).

Stone columns may not be appropriate in very soft soils that do not provide enough lateral confinement to the columns. In those cases, a proper shape of the column cannot be ensured during installation and excessive deformation is expected upon loading. An undrained shear strength of the soft soil of around 5-15 kPa (Wehr, 2006) is generally adopted as the limit value to define stone column feasibility. To increase the lateral confinement of the columns, and consequently, their vertical capacity, encasing the columns with geotextiles or other geosynthetics has been a successful solution in recent years (Alexiew and Raithel, 2015). Using horizontal geosynthetic disks placed in regular vertical intervals through the column length has also shown to be an efficient alternative (e.g. Ali et al., 2012 and 2014; Hosseinpour et al., 2014; Sharma et al., 2004).

Stone columns and encased stone columns (ESC) are typically employed under embankments or large uniformly loaded areas (e.g. Almeida et al., 2015; Chen et al.,

2015; Fattah et al., 2016; Yoo, 2016). In those cases, columns are distributed in a large regular mesh and the problem is usually simplified to a "unit cell", i.e. only one granular column, its encasement, if present, and the corresponding surrounding soil. The large number of columns justifies symmetry boundary conditions. So, the lateral boundary of the “unit cell” is rigid, frictionless and shear free. The simplicity of the model allows for analytical solutions that provide the settlement reduction (e.g. Priebe, 1995; Raithel and Kempfert, 2000; Pulko et al., 2011; Castro and Sagaseta, 2013).

More recently, stone columns have also been deployed beneath small isolated pad or strip footings at low or moderate loading conditions (e.g. Watts et al., 2000). Several authors (e.g. Wood et al., 2000; Castro, 2014) have studied the bearing capacity and deformations of these groups of stone columns. The columns under pad or strip footings may also be encased, if necessary, forming groups of ESC. However, there is little information about the performance of these groups of ESC (Murugesan and Rajagopal, 2010; Raithel et al., 2011; Keykhosropur et al., 2012) as most studies focus on the behaviour of single ESC (e.g. Malarvizhi and Ilamparuthi, 2007) or very large groups, analysing only a “unit cell” (e.g. Lo et al., 2010). To the best of the author’s knowledge, there is no published research on the influence of the arrangement of ESC, i.e. number of columns and column position, beneath a rigid footing. Besides, many papers use the column length to diameter ratio, for example, to give the critical column and encasements lengths (e.g. Malarvizhi and Ilamparuthi, 2007; Ali et al., 2012). This paper shows that the column length to diameter ratio has a minor effect and, for example, the critical column and encasement lengths should be given as a function of the footing diameter or width, which is the parameter that mainly controls the

131 deformation mode.

132

133 To evaluate the performance of groups of ESC beneath rigid footings (circular or
134 square), a set of systematic 2D and 3D finite element analyses have been carried out.
135 These numerical simulations aim to show that, if the total column cross-sectional area
136 and the ratio between encasement stiffness and column radius are kept constant, the
137 column arrangement, i.e. column position and number of columns, has a minor
138 influence on the settlement reduction. That allows for a simplified two-dimensional
139 model in axial symmetry of groups of ESC beneath a rigid footing. Besides, the critical
140 column and encasement lengths are analysed. So, the paper presents firstly a
141 dimensional analysis in Section 2 to identify the main variables of the problem and the
142 corresponding dimensionless parameters. Next, the numerical models are presented
143 (Section 3). A common case is used as a reference, and using that case as a basis,
144 parametric studies are performed. The results are discussed in Section 4, showing, for
145 example, the small influence of column position within the group. That is confirmed by
146 a reanalysis of previous experimental data in Section 5 and some summarizing
147 comments on column arrangement are presented in Section 6. Using the presented
148 numerical models, the critical column and encasement lengths are evaluated in Section
149 7. Finally, some conclusions are derived.

150

151 **2. DIMENSIONAL ANALYSIS**

152 Firstly, the variables of the problem are identified and a dimensional analysis is
153 performed to get them in a dimensionless form. This dimensional analysis simplifies the

154 parametric study and helps extrapolating the results of the numerical analyses presented
155 in this paper. The variables of the problem may be classified as follows:

156 (a) Geometrical variables: Footing width, B; soft soil layer thickness, H; column
157 length, L_c; encasement length, L_g; column radius, r_c; centre-to-centre column
158 spacing, s; number of columns beneath the footing, N, and column position.

159 (b) Initial stress state (e.g., p'_0, K_0) and applied vertical pressure on the footing, p_a.

160 (c) Soil, column and encasement properties: stiffness and strength.

161 (d) Results, e.g., settlement, s_z.

162

163 As the encasement thickness is usually negligible, its radius corresponds to that of the
164 column, r_c. The encasement length, L_g, may be normalised by that of the column, L_g/L_c,
165 but this paper will show that, for groups of columns, L_g/B is more meaningful. The other
166 geometrical variables are the same as those of groups of non-encased stone columns.
167 They have been analysed in detail in Castro (2014) and only five of them are
168 independent. The following dimensionless variables are used here: H/B, L_c/B, a_r, N and
169 the column position. a_r is the area replacement ratio, which is a crucial dimensionless
170 parameter that provides the percentage of soft soil replaced by gravel, i.e. a_r is the area
171 of the columns, A_c, divided by the loaded area, A_l. Here, all the columns will be
172 assumed to be beneath the footing because it is generally more efficient (Wehr, 2004).
173 Additional columns beyond the footing increase the bearing capacity but do not
174 noticeably reduce the footing settlement (e.g. Wood et al., 2000; Castro, 2014). It is
175 worth noting that the footing width (B) or diameter plays an important role and some
176 authors (e.g. Hong et al., 2016) seem to overlook its influence. On the contrary, L_c/d_c is

177 commonly used (e.g. Dash and Bora, 2013) but it will be shown here that its influence is
178 negligible.

179

180 The soil properties depend on the constitutive model but they are either dimensionless
181 or have units of pressure. The latter ones are typically normalised using the initial stress
182 state (e.g. c_u/p'_0). The applied vertical pressure may be normalised using either the
183 initial stress state or a soil property (e.g. p_a/c_u). The column properties that have units
184 are usually normalised by the soil corresponding ones (e.g. the stiffness modular ratio
185 E_c/E_s).

186

187 The encasement is usually assumed to behave as a linear elastic material because its
188 strength is typically high enough. A theoretical analysis of the encasement behaviour
189 (e.g. Pulko et al., 2011) shows that the influence of the encasement stiffness, J_g, is given
190 by the following dimensionless parameter $J_g/(r_c E_{oed,s})$, where $E_{oed,s}$ is the oedometric
191 (confined) stiffness of the surrounding soil. That is valid for an elastic behaviour of the
192 surrounding soft soil; if significant plastic strains develop in the surrounding soil, it is
193 more appropriate to use a strength parameter, e.g. c_u, instead of the soil stiffness.

194

195 Finally, the settlement for a given applied pressure, p_a, is commonly related to the
196 settlement without columns, i.e. the settlement reduction factor, $\beta = s_z / s_{z0}$, to highlight
197 the improvement achieved with the column treatment.

198

3. NUMERICAL MODELS

Numerical simulations were performed to provide a better understanding of the performance of ESC beneath rigid footings (circular and square). The footing settlement and the stresses on soil, column and encasement were analysed. The study started with a simple reference case and parametric studies were performed. In a previous publication (Castro, 2014), the author showed that for non-encased stone columns, the number of columns has a negligible influence, if a_r is kept constant. Here, the same will be shown for ESC, if a_r and J_g/r_c are kept constant. The influence of the column and encasement length will be also investigated.

3.1 Numerical code and basic assumptions

The finite element codes Plaxis 3D 2013 (Brinkgreve et al., 2013) and Plaxis 2D 2015 (Brinkgreve et al., 2015) were used for the full 3D models and the simplified 2D axisymmetric models, respectively. The soft soil and the stone columns were modelled as continuum elements using 10-node tetrahedral elements for the 3D cases and 15-node triangular elements for 2D. The geosynthetic encasement was modelled as elements that have only normal stiffness, i.e. they only have translational degrees of freedom at their nodes, and can only sustain tensile stresses. In 2D, a 5-node line element was used, whereas a 6-node triangular surface element was used in 3D. Perfect bonding between soil, columns and their encasements at their interfaces was modelled, as it is common practice (e.g. Keykhosropur et al., 2012), because they are tightly interlocked. The rigid footing was assumed as perfectly rough and modelled as a very stiff plate that produces uniform settlements. The finite elements for the footing were 6-node triangular elements

222 in 3D and 5-node line elements in 2D. Those elements have translational and rotational
223 degrees of freedom and their properties are the flexural rigidity and the normal stiffness.
224
225 All the numerical simulations were performed using a small strain formulation and a
226 staged construction process was modelled. Initially, the natural soft soil was modelled
227 with a horizontal ground surface and a constant thickness. Geostatic initial stresses were
228 generated using the soil unit weight and the coefficient of lateral earth pressure at rest,
229 K_0. Later, the footing and the columns with their corresponding encasements were
230 "wished-in-place", ignoring the changes in the natural soil due to column construction
231 (Castro and Karstunen, 2010). Finally, the loading on the footing was simulated.
232 Drained conditions were assumed for all the process, i.e. no excess pore pressures were
233 generated. Consequently, the response was studied in effective stresses. That is because
234 this paper does not focus on the stability but on the long-term settlement, as soft soils
235 can undergo large settlements at relatively low loads and the serviceability limit state
236 may be critical for the design (e.g., Black et al. 2011, McCabe and Killeen, 2016).
237

238 **3.2 Reference case**

239 The reference case consists of only one ESC under the centre of a square rigid footing.
240 The footing width, B, is 5 m and the column diameter (d_c=1.78 m) was chosen to give
241 an area replacement ratio of a_r=10%. The value of a_r=10% may be low for a small
242 footing but it has been chosen to have a broad range of variation of column spacing and
243 number of columns for the parametric analyses. The column diameter is also high, but it
244 was chosen to have more realistic column diameters when using more realistic number

245 of columns beneath the footing (see Table 1). The column is considered to reach a rigid
246 substratum at 10 m depth. So, the column is end-bearing (L_c/H=1) and has a length of
247 L_c=10 m. The encasement was assumed to cover the full length of the column
248 (L_g=L_c=L). To take advantage of the symmetry of the problem, only a quarter is
249 modelled (Figure 1). The symmetry would allow for further reduction, but that is not
250 useful in this particular numerical code. Sensitivity analyses were performed to study
251 the model dimensions and a ratio of model to footing breadth of 6 was considered
252 enough. The bottom boundary is fixed and roller vertical conditions are assumed for the
253 lateral boundaries.

254

255 It is worth noting that this reference case is not equivalent to the isolated stone column
256 that is considered in many studies (e.g. Murugesan and Rajagopal, 2006) because in
257 those cases the load is applied only on top of the column, which means an a_r=100% and,
258 it is generally less efficient at reducing the settlement, yet it is useful for field load tests.

259

260 Common soil, column and encasement properties (Table 2) were used for the idealised
261 case analysed in this paper (e.g. Barksdale and Bachus, 1983; Alexiew and Raithel,
262 2015). The soil profile was simplified to only one homogeneous soil layer. An elastic-
263 perfectly plastic behaviour was considered for the soil and column using the Mohr-
264 Coulomb yield criterion and a non-associated flow rule, with a constant dilatancy angle.
265 A Poisson's ratio of ν_s=ν_c=0.33 was assumed for the soil and column and their Young's
266 moduli were taken as E_s=2 MPa and E_c=30 MPa, respectively. That means a modular
267 ratio of 15. Although the crushed stone (gravel) used for the column backfill is a pure
268 frictional material, a small cohesion (c_c=0.1 kPa) was used to avoid numerical problems.

Typical values of ϕ_c=40º and ψ_c =5º were chosen for the gravel. For the soft soil, representative cohesion and friction angle (c_s=3 kPa and ϕ_s=23º) were assumed within the common range. The soil was considered as a non-dilatant material. A stiffness of J_g=2000 kN/m was taken for the geosynthetic encasement and a null Poisson's ratio (ν_g=0) because the geosynthetic encasement was assumed to have two major directions (radial and longitudinal), which behave independently (e.g. Soderman and Giroud, 1995; Castro, 2016).

A uniform vertical pressure of p_a=100 kPa was applied on the rigid footing. This applied pressure is high enough to produce significant plastic strains. For the sake of simplicity, the ground water level was assumed to be at the ground surface and an effective unit weight of γ'=10 kN/m^3 for soil and column was directly considered without modelling pore water pressures. The coefficient of lateral earth pressure at rest was set equal to K_0=0.6, using the Jaky's formula for the soil and disregarding installation effects.

3.3 Parametric studies

Using the reference case as a starting point, parametric studies were carried out varying several properties:

(a) Column arrangement. The number of columns, N, the centre-to-centre column spacing, s, and their positions were varied. Typical column configurations were used. For the sake of comparison, the number of columns was varied without changing the area replacement ratio, a_r, and consequently, the diameter of the columns is obtained

using a_r, N and B. The J_g/d_c ratio was also kept constant. So, depending on the number of columns, the encasement stiffness was varied to get the same J_g/d_c ratio as in the reference case.

(b) Other geometric factors. The size of the footing B, the length of the encasement and columns L_g, L_c, the soft soil layer thickness H and the area replacement ratio, a_r.

(c) Material properties. In the previous parametric studies, the normalised encasement stiffness was varied from a null value, i.e. no encasement, to a high enough value. Besides, a specific parametric study of the strength of the soil was also performed. Other column or soil parameters, such as their stiffnesses, were not varied because of their less important effect.

3.4 Mesh sensitivity analyses

Some mesh dependency was foreseen due to the problem configuration, i.e. a rigid footing in a 3D mesh. A preliminary analysis of several column groups confirmed a slight mesh dependency. Due to computational restrictions, the number of elements is limited in the 3D mesh. Therefore, for the mesh sensitivity analyses, the square footing was changed to a circular one with the same area to have axial-symmetry and model the problem also in a fine enough 2D mesh (Figure 2). In fact, the main improvement in the 2D simulations is not caused by the number of elements but by their higher order (i.e. 15-node triangular elements in 2D and 10-node tetrahedral elements in 3D for soil and column elements).

The results of the mesh sensitivity analyses are summarized in Figure 3, where the settlement simulated using the 3D mesh is compared with that using the fine enough 2D mesh. For each number of elements, the most accurate mesh was also searched, i.e. refining the mesh in the area of interest (footing, column and encasement) and using a coarse mesh in the far field (Figure 1). For all the parametric studies, it was decided to use comparable meshes of around 65-75 thousand elements with the same degree of relative refinement. Although those meshes slightly underpredict the settlement (around 5%), they are perfectly valid to compare and identify trends in the parametric studies.

4. RESULTS AND DISCUSSION

4.1 Column position

The first parametric study focused on the influence of column spacing, or more precisely, the relative position of the columns beneath the footing. A group of four stone columns (N=4) was used, keeping constant the area replacement ratio of the reference case (a_r=10%) and the J_g/d_c ratio; so, d_c=0.89 m and J_g=1000 kN/m. The spacing between columns was varied from s=1 to 4 m (Figure 4). Besides, two additional encasement stiffnesses were studied, namely no encasement (J_g=0) and J_g=2500 kN/m. The settlements of the groups of non-encased and encased columns (N=4) were compared with the settlements of the cases with a single column (N=1) and similar results were found (Figure 5). On one hand, the settlement is slightly higher when the columns are close to the edges of the footing for the non-encased columns and on the other hand, the settlement is lower for the encased columns when the columns are close to the footing edges. The two main effects that control the influence of the column

338 position on the settlement reduction are:

339 – when the columns are close to the edges, they tend to support higher vertical
340 stresses because the stresses are higher at the edges for a rigid footing;

341 – when the columns are close to the centre, the surrounding vertical and horizontal
342 stresses are higher and, therefore, the columns are better laterally confined.

343

344 Both effects mostly balance each other out, but depending on the soil, column and
345 encasement properties one may be slightly more beneficial than the other (Figure 5). For
346 the encased columns, if they are close to the edges (s=4 m), they support higher vertical
347 stresses than those close to the centre (s=1 m) (Figure 6). For the non-encased columns
348 (J_g=0), the positive effect of positioning the columns close to the edges disappears
349 because their lateral support is lower and their lateral expansions cause a slight increase
350 in the settlement (Figure 5).

351

352 Column position has a small influence on the settlement of groups of encased columns.
353 However, the maximum circumferential or hoop tensile force of the encasement (F_g)
354 notably increases when the columns are close to the footing edges (Figure 7), e.g. from
355 14.5 to 22.8 kN/m for column spacings of s=1 and 4 m, respectively. As previously
356 mentioned, the vertical stresses are higher near the edges of a rigid footing and that
357 cause a higher maximum of the tensile encasement force F_g, when the columns are close
358 to the footing edges. Figure 7 shows the circumferential tensile force of the encasement
359 for a diagonal cross section and at the outer boundary. Although the tensile force F_g is
360 slightly higher at the outer boundary than at the inner boundary, F_g is quite similar all
361 around the encasement for the same depth. The fact that a greater maximum F_g

362 develops, when the columns are close to the footing edges, could lead to think that in
363 those cases the encasement contribution is more important and then, the settlement is
364 further reduced. However, that is not the case, since the average F_g of the encasement is
365 similar for different spacings (Figure 7).

366

367 The depth of maximum F_g depends of the column mode of deformation, and this, in
368 turn, depends on the encased column position. So, in this case, for a column spacing of
369 s=1 m, the maximum F_g is located at 3 m depth, i.e. z/B=0.6, because bulging is the
370 main mode of deformation for centre columns. On the other hand, for columns close to
371 the footing edges, shearing is the main mode of deformation, and the maximum F_g
372 occurs at shallow depths, e.g. at 0.7 m depth for s=4 m. The zones of maximum
373 shearing and bulging within the columns are directly related to the deformation beneath
374 a rigid footing (Figure 8 and Figure 9).

375

376 **4.2 Number of columns**

377 The next parametric study focused on the influence of the number of columns, which
378 was varied between N=1 and 24 in multiples of 4 to retain the symmetry. The variation
379 of the number of columns inevitably leads to some changes in the column position. To
380 reduce that influence, all the columns were uniformly placed along a square with a side
381 length of 4 m. Besides, two different column configurations were used, one with a
382 column at the corner of the square and another with columns just on the sides (Figure
383 10). The diameter of the columns (d_c) and the encasement stiffness (J_g) were varied
384 accordingly to keep a_r and J_g/d_c constant (Table 1).

385

386 The results show the small influence of the number of columns on the settlement
387 reduction (Table 3). There are some differences but they may be attributed mainly to the
388 differences in the column position because they follow the same trends as those in the
389 previous section. It is worth noting that for each number of columns, the ratio L/d_c is
390 different (from roughly 5 up to 27) because a_r=10% is kept constant. That demonstrates
391 the minor influence of the L/d_c ratio on the settlement reduction for a constant
392 normalised encasement stiffness (J_g/d_c). Just for very high values of the L/d_c ratio, i.e.
393 very slender columns, there may appear second order effects or low-quality finite
394 elements.

395

396 Contrary to the settlement reduction, the maximum hoop force at the encasement (F_g)
397 notably changes (Table 4). The differences are mainly caused by the varying stiffness of
398 the encasement for different number of columns (Table 1). The encasement was
399 assumed to behave as a linear elastic material; so, it may be easily demonstrated that
400 F_g=J_g ε_r , where ε_r is the radial strain. In this way, the hoop force may be normalised by
401 the encasement stiffness (F_g/J_g). Those normalised values are not affected by the
402 number of columns, N (Table 5). However, F_g/J_g notably varies with many other
403 factors, such as column position, normalised encasement stiffness (J_g/d_c) or surrounding
404 soil strength.

405

406 It is worth noting that the hoop force at the encasement (F_g) may oscillate due to strain
407 localization as pointed out by Pulko et al. (2011) and Castro and Sagaseta (2011).
408 Besides, the hoop force, and particularly its maximum value, is more mesh sensitive

409 than the settlement.

410 **4.3 Soil properties**

411 As already mentioned, only the strength of the soil was altered because other column
412 and soil parameters, such as their stiffnesses, have a less important effect. Small
413 differences were found in the settlement reduction between different column
414 configurations (Table 6a) except for the softest soil (ϕ_s=20º ; c_s=1 kPa), which is not a
415 desired case because of the large zone at failure (Figure 11). The soil strength affects the
416 two commented phenomena related to column position. So, an encased column usually
417 reduces the settlement further if placed near the footing edges. This effect is more
418 pronounced if the surrounding soil is very soft. On the other hand, the hoop forces at the
419 encasement are notably higher (Table 6b).

420

421 **4.4 Soil layer thickness and footing width**

422 The soil layer thickness was varied to study its influence on the settlement reduction
423 (Table 7). For end-bearing columns (L=H), that is analogous to vary the footing width
424 because the ratio H/B is the governing parameter. In fact, H/B indicates the extension of
425 the load and whether it is a small footing or a large loaded area that can be studied using
426 the "unit cell" concept. When H/B decreases and the columns are not near the footing
427 edges, the lateral confinement of the columns improves. So, the slight positive effect of
428 positioning the columns near the footing edges for H/B=2 (reference case) vanishes for
429 H/B=1.2 (similar settlement for different column spacings). For values of H/B lower
430 than 1.2, positioning the columns beneath the centre of the footing gives slightly less
431 settlement (Table 7).

4.5 Column length

So far, only end-bearing columns had been modelled ($L=H$). Now, the column and encasement lengths were reduced to study their influence (Figure 12). For the sake of simplicity, the floating columns are assumed to be fully encased, i.e. $L=L_g=L_c$. For floating columns, the column position is slightly more relevant than for end-bearing columns because there is a new effect:

- Column punching or penetration into the underlying soil, which is related to the deformation of the soil layer that is not improved beneath the columns.

For the same area replacement ratio, column penetration into the underlying soil is greater when there is less number of columns and with closer spacings (Figure 12 and Table 8). In this regard, the behaviour is similar to that of non-encased columns (Wood et al., 2000; Castro, 2014), where column penetration is greatest when the columns are in the middle of the footing, they are short and a_r is high. When the column tip is near the vertex of the pyramid created by the maximum shear strain contours, the column notably punches into the underlying soil, e.g. for a central column and L/B around 1 (Figure 8c and Figure 9). Therefore, columns near the edges give slightly less settlement than central columns for those column lengths ($L \approx B$) (Figure 12).

The number of columns has less influence on the settlement reduction than their position (Table 8). Nevertheless, an increasing number of columns reduces the column punching because it distributes the load on the underlying layer; therefore, slightly less

455 settlement is computed.

456

457 In summary, when floating columns reach a critical length (for example, L=8 m in this
458 case), their behaviour is similar to that of end-bearing columns. If they are shorter,
459 distributing the columns beneath the footing (more columns and near the footing edges)
460 gives slightly less settlement. Yet, the differences are not very important, namely
461 smaller than 20% (Figure 12 and Table 8).

462

463 **4.6 Area replacement ratio**

464 The value of a_r=10% may be low for a small footing because it has been chosen to have
465 a broad range of variation of column spacing and number of columns. So, the study was
466 extended to higher values of a_r, namely 20% and 30%. The results (Table 9) show
467 similar trends to those obtained with a_r=10%. Only two subtle differences were found:

468 – For end-bearing columns (L=H=2B), the slight beneficial effect of positioning
469 the columns near the footing edges (e.g., s=3 m) vanishes for higher area
470 replacement ratios (e.g., a_r=30%). In the present analysis, the encasement
471 stiffness was kept constant for different area replacement ratios and then, its
472 contribution to the lateral confinement of the column is lower for higher area
473 replacement ratios.

474 – For floating columns (L=B), the punching of the columns slightly increases with
475 the area replacement ratio, as already mentioned and similarly to non-encased
476 columns (Wood et al., 2000).

5. ANALYSIS OF PREVIOUS EXPERIMENTAL DATA

It is difficult to find previous experimental data in the literature that allow to study the influence of the column arrangement beneath a rigid footing. Ali et al. (2014) compare the results of laboratory small-scale tests on single and groups of encased columns. The advantage of this case is that the area replacement ratio beneath the footing and the column diameter are roughly the same in both cases.

The analysis of those data (Figure 13) shows that the results for a single column and for a group of three columns are very similar, which confirms the small influence of the column arrangement beneath a rigid footing. It is worth noting that there are differences between both cases: the footing diameter is 60 mm for the single column and 96 mm for the group of columns and the area replacement ratio is 25% for the single column and 29% for the group of columns. For the group of columns, there are also extra column outside the footing. However, these differences nearly compensate between each other, being the settlement for the single column slightly lower due to the smaller footing dimensions. For the case without encasement, the results of a single column and footing diameter of 100 mm (Ali et al., 2012) are also included to show that in this case the settlement is higher due to the bigger footing diameter. It is worth noting that Ali et al. (2014) seem to neglect the influence of the footing width (B) and also that the effect of the encasement is controlled by the parameter J_g/d_c and then, the results for the same type of encasement but with different column diameter are not comparable.

6. COMMENTS ON COLUMN ARRANGEMENT

This paper shows the small influence of column arrangement in groups of ESC beneath a rigid footing on the reduction of settlement achieved with a ESC treatment. Similar results were found for the full 3D model and for the 2D axisymmetric model with an equivalent central column that keeps both a_r and J_g/d_c (Figure 2 and Table 1). Besides, the central column generally gives results on the safe side (e.g. Table 6a) and the 2D mesh is less computational demanding and generally uses more elements of higher order, providing more accurate results. That "one column" model may be useful not only for numerical analyses but also for analytical approaches.

In practise, uniformly distributed columns beneath the footing is the usual configuration. The small influence of the column arrangement on the settlement reduction found in this paper justifies that construction practise, because uniformly distributed columns are more beneficial for some other factors not included in this study, such as bending moments in the footing, soil drainage and easiness of construction.

7. CRITICAL COLUMN AND ENCASEMENT LENGTHS

The simplified model of only one column is used here to investigate the critical or optimal column and encasement lengths. For non-encased stone columns, there is a critical length of the columns around 1.5-2B for settlement reduction (Wehr, 2004; Castro, 2014). It is worth noting that many authors (e.g. Malarvizhi and Ilamparuthi,

2007; Ali et al., 2012) give critical lengths as a function of the column diameter, but as it has been here shown (Table 3), the column length to diameter ratio has a minor influence by itself. For settlement reduction, the critical column length is related to the pressure bulb that the footing generates (Figure 14a), and for footing bearing capacity, the critical length depends on the failure mechanism (Figure 14b). As the critical length for settlement reduction is longer, that is usually the considered value. For large loaded areas (high values of B), the critical column length is higher than the soft layer thickness, and consequently, the concept of critical or optimal length does not apply. For encased columns, Figure 15 shows that the critical length of fully encased columns varies between 1.9-3.3B for the studied cases. These values are higher than for non-encased columns because the columns are better laterally confined and transmit the load deeper. For the reference case (Figure 15a, dashed lines), the rigid bottom is not far enough (H/B=2) to clearly identify the critical length. Therefore, the size of the footing was reduced (H/B=4) to better illustrate the critical length of the column (solid lines).

In the present case, there are important plastic strains and the critical length of the column is related to the extent of those plastic strains with depth (Figure 16). The critical length of the column is slightly lower for higher area replacement ratios (Figure 15a, solid lines) because the extent of the plastic strains decreases with a_r, i.e. 2.6B for a_r=10%, 2.4B for a_r=20% and 2.3B for a_r=50% (Figure 16).

The critical length of the column depends on the problem variables, e.g. the strength of the surrounding soft soil. For a higher strength of the surrounding soft soil (c_s=10 kPa and ϕ_s=30º), the plastic strains are reduced and also their extent with depth.

546 Consequently, the critical column length is lower (1.9B), but the elastic strains below
547 the column tip are relatively more significant (Figure 15b). On the other hand, the
548 encasement stiffness also plays an important role because, for higher encasement
549 stiffnesses (e.g. J_g=5000 kN/m), the applied load is transferred to deeper layers, and
550 consequently, the critical column length is higher (2.5-3.3B in this case, Figure 15c).

551

552 The previous analyses are for fully encased stone columns, i.e. (L_g=L_c) that do not
553 necessarily reach a rigid stratum (L<H). Some authors (e.g. Murugesan and Rajagopal,
554 2006, 2007) have proposed to partially encased the columns. Murugesan and Rajagopal
555 (2006, 2007) studied isolated columns, i.e. B=d_c and a_r=100%, and found a critical
556 encasement length of L_g=2-3d_c=2-3B. Yoo (2010) already noted that the critical
557 encasement length depends strongly on the loading type and found that for embankment
558 loading there was not a critical depth and confirmed the results of Murugesan and
559 Rajagopal (2006, 2007) for isolated column loading. Castro et al. (2013) also found
560 using analytical solutions that for embankment loading, there is not a sharp change in
561 reducing the settlement when varying the encasement length.

562

563 To analyse the critical length of the encasement, columns that reach a rigid substratum
564 (L_c=H) but are partially encased (L_g<L_c) were numerically simulated. The results
565 (Figure 17) show that there is a critical length for the encasement that varies between
566 1.4 and 2.8B for the analysed cases. The critical length of the encasement also depends
567 on the pressure bulb generated by the footing; so, the length of the encasement was also
568 normalised by the footing width, L_g/B. The critical length of the encasement is slightly
569 lower than that of the column because it is related to the extent of the plastic strains just

570 in the surrounding soil (Figure 16). For the reference case, those values are 1.9*B* for
571 a_r=10%, 1.7*B* for a_r=20% and 1.4*B* for a_r=50%. The critical length of the encasement is
572 slightly reduced for higher strengths of the surrounding soil (Figure 17b) and increases
573 for higher encasement stiffnesses (Figure 17c).

574

575 In conclusion, the critical column and encasement lengths are mainly controlled by the
576 size of the footing, *B*. The critical length of the columns is 1.5-2 *B* for non-encased
577 columns, these values are higher for encased columns (around 2-3.5*B,* higher values for
578 higher encasement stiffnesses) because encased columns transfer the load deeper. On
579 the other hand, the critical length of the encasement is only slightly lower than that of
580 the column (around 1.5-3*B*). So, in most cases where partially encasing the column is
581 effective, reducing the total column length would be more economical.

582

CONCLUSIONS

The paper presents a set of systematic numerical analyses of groups of encased stone columns beneath a rigid footing. If the area replacement ratio (a_r) and the normalised encasement stiffness (J_g/d_c) are the same, the column arrangement (both column position and number of columns) has a small influence on the settlement reduction. The column position is slightly more relevant than the number of columns because of the following two effects:

1) Near the edges of a rigid footing, the vertical stresses are higher, so columns near the edges would tend to support higher loads.
2) On the contrary, columns beneath the center are better laterally confined.

Both effects tend to balance each other out, but depending on the case, one may be slightly more beneficial than the other.

For floating columns, there appears a third effect:

3) Column punching or penetration into the underlying soil.

This effect causes further differences between different column arrangements but disappears once the column length is higher than a critical or optimal one.

The small influence of the column arrangement on the settlement reduction may allow for a 2D axisymmetric model with an equivalent central column that retains both a_r and J_g/d_c.

605 In a homogeneous soil layer, encased columns beneath a rigid footing have a critical
606 length of around 2-3.5*B* for settlement reduction. The critical length depends on the
607 extent of plastic strains, increases with the encasement stiffness and decreases with the
608 area replacement ratio and the soil strength.

609

610 The critical length of the encasement for partially encased column is slightly lower
611 (around 1.5-3*B*), depends on the plastic strains in the surrounding soft soil and also
612 increases with the encasement stiffness and decreases with the area replacement ratio
613 and the soil strength.

614

615 The presented analysis is mainly based on finite element simulations; further
616 experimental investigation is necessary to confirm the above conclusions.

617

REFERENCES

Alexiew, D., Raithel, M., 2015. Geotextile-Encased Columns: Case Studies over Twenty Years, in: Indraratna, Chu, Rujikiatkamjorn (Eds.), Embankments with Special Reference to Consolidation and Other Physical Methods. Butterworth-Heinemann, pp. 451-477.

Ali, K., Shahu, J.T., Sharma, K.G., 2012. Model tests on geosynthetic-reinforced stone columns: a comparative study. Geosynth. Int. 19 (4), 433-451.

Ali, K., Shahu, J.T., Sharma, K.G., 2014. Model tests on single and groups of stone columns with different geosynthetic reinforcement arrangement. Geosynth. Int. 21 (2), 103-118.

Almeida, M., Hosseinpour, I., Riccio, M., and Alexiew, D., 2015. Behavior of Geotextile-Encased Granular Columns Supporting Test Embankment on Soft Deposit. J. Geotech. Geoenviron. Eng. 141(3), 04014116.

Barksdale, R.T., Bachus, R.C., 1983. Design and construction of stone columns. Report FHWA/RD-83/026. Nat Tech Information Service, Springfield.

Black, J.A., Sivakumar, V., Bell, A., 2011. The settlement performance of stone column foundations. Géotechnique 61(11), 909-922.

Brinkgreve, R.B.J., Engin, E., Swolfs, W.M., 2013. Plaxis 3D 2013 Manual. Plaxis bv, the Netherlands.

Brinkgreve, R.B.J., Kumarswamy, S., Swolfs, W.M., 2015. Plaxis 2D 2015 Manual. Plaxis bv, the Netherlands.

Castro, J., 2014. Numerical modelling of stone columns beneath a rigid footing. Comput. Geotech. 60, 77-87.

Castro, J., 2016. Discussion of "Column Supported Embankments with Geosynthetic Encased Columns: Validity of the Unit Cell Concept". Geotech. Geol. Eng. 34(1), 419-420.

641 Castro, J., Karstunen, M., 2010. Numerical simulations of stone column installation. Can.
642 Geotech. J., 47(10), 1127-1138.

643 Castro, J., Sagaseta, C., 2011. Deformation and consolidation around encased stone columns.
644 Geotext. Geomembr. 29, 268-276.

645 Castro, J., Sagaseta, C., 2013. Influence of elastic strains during plastic deformation of encased
646 stone columns. Geotext. Geomembr. 37, 45-53.

647 Castro, J., Sagaseta, C., Cañizal, J., Da Costa, A., Miranda, M., 2013. Foundations of
648 embankments using encased stone columns. Proc. 18th Int. Conf. Soil Mech. Geotech.
649 Eng., Vol. 3, pp. 2445-2448. Paris, France.

650 Chen, J.-F., Li, L.-Y., Xue, J.-F., Feng, S.-Z., 2015. Failure mechanism of geosynthetic-encased
651 stone columns in soft soils under embankment. Geotext. Geomembr. 43(5), 424-431.

652 Dash, S.K., Bora, M.C., 2013. Influence of geosynthetic encasement on the performance of
653 stone columns floating in soft clay. Can. Geotech. J. 50(7), 754-765.

654 Fattah, M., Zabar, B., and Hassan, H., 2016. Experimental Analysis of Embankment on
655 Ordinary and Encased Stone Columns. Int. J. Geomech. 16(4), 04015102.

656 Hong, Y.-S., Wu, C.-S., Yu, Y.-S., 2016. Model tests on geotextile-encased granular columns
657 under 1-g and undrained conditions. Geotext. Geomembr. 44(1), 13-27.

658 Hosseinpour, I., Riccio, M., Almeida, M.S.S., 2014. Numerical evaluation of a granular column
659 reinforced by geosynthetics using encasement and laminated disks. Geotext. Geomembr.
660 42(4), 363-373.

661 Keykhosropur, L., Soroush, A., Imam, R., 2012. 3D numerical analyses of geosynthetic encased
662 stone columns. Geotext. Geomembr. 35, 61-68.

663 Lo, S.R., Zhang, R., Mak, J., 2010. Geosynthetic-encased stone columns in soft clay: a
664 numerical study. Geotext. Geomemb. 28 (3), 292-302.

665 Malarvizhi, S.N. Ilamparuthi, K., 2007. Comparative study on the behaviour of

encased stone column and conventional stone column. Soils Found. 47(5), 873–885.

McCabe, B.A., Killeen, M.M., 2016. Small Stone-Column Groups: Mechanisms of Deformation at Serviceability Limit State. Int. J. Geomech. 2016; 0406114.

Murugesan, S., Rajagopal, K., 2006. Geosynthetic-encased stone columns: Numerical evaluation. Geotext. Geomem. 24(6), 349–358.

Murugesan, S., Rajagopal, K., 2007. Model tests on geosynthetic encased stone columns. Geosynthet. Int. 14(6), 346–354.

Murugesan, S. Rajagopal, K., 2010. Studies on the Behavior of Single and Group of Geosynthetic Encased Stone Columns. J. Geotech. Geoenviron. Eng. 136(1), 129–139.

Priebe, H.J., 1995. Design of vibro replacement. Ground Eng. 28(10), 31-37.

Pulko, B., Majes, B., Logar, J., 2011. Geosynthetic-encased stone columns: Analytical calculation model. Geotext. Geomembr. 29(1), 29-39.

Raithel, M., Kempfert, H.G., 2000. Calculation models for dam foundations with geotextile coated sand columns. In: Proceedings of the International Conference on Geotechnical & Geological Engineering, GeoEngg—2000, Melbourne.

Raithel, M., Werner, S., Küster, V., Alexiew, D., 2011. Analyse des Trag- und Verformungsverhaltens einer Gruppe geokunststoffummantelter Säulen im Großversuch. Bautechnik 88, Heft 9, 593-601.

Sharma, S.R., Phanikumar, B.R., Nagendra, G., 2004. Compressive load response of granular piles reinforced with geogrids. Can. Geotech. J. 41 (1), 187–192.

Soderman, K.L., Giroud, J.P., 1995. Relationships between uniaxial and biaxial stresses and strains in geosynthetics. Geosynth. Int. 2(2), 495-504.

Watts, K.S, Johnson, D., Wood, L.A., Saadi, A., 2000. An instrumented trial of vibro ground treatment supporting strip foundations in a variable fill. Géotechnique 50(6), 699-708.

690 Wehr, J., 2004. Stone columns – single columns and group behaviour. Proc. 5th Int. Conf.
691 Ground Improvement Tech., Kuala Lumpur, pp. 329-340.

692 Wehr, J., 2006. The undrained cohesion of the soil as criterion for the column installation with a
693 depth vibrator. In: Proceedings of the International Symposium on vibratory pile driving
694 and deep soil vibratory compaction, TRANSVIB 2006, Paris.

695 Wood, D.M., Hu, W., Nash, D.F.T., 2000 Group effects in stone column foundations: model
696 tests. Géotechnique 50(6), 689-698.

697 Yoo, C., 2010. Performance of Geosynthetic-Encased Stone Columns in Embankment
698 Construction: Numerical Investigation. J. Geotech. Geoenviron. Eng. 136(8), 1148–1160.

699 Yoo, C., 2016. Settlement behavior of embankment on geosynthetic-encased stone column
700 installed soft ground – A numerical investigation. Geotext. Geomembr. 43(6), 484-492.

701

702

703 **TABLE CAPTIONS**

704 Table 1. Column diameter and encasement stiffness for different number of columns.

705 Table 2. Soft soil and column properties for reference case

706 Table 3. Settlement (mm) for different number of columns.

707 Table 4. Maximum hoop force at the encasement, F_g (kN/m), for different number of
708 columns.

709 Table 5. Normalised maximum hoop force at the encasement, F_g/J_g (%), for different
710 number of columns.

711 Table 6. Results for different soil material strengths. Reference case: (a) Settlement
712 (mm); (b) Maximum hoop force at the encasement (kN/m).

713 Table 7. Settlement (mm) for different soil layer thicknesses.

714 Table 8. Results for different column lengths. Reference case: (a) Settlement (mm); (b)
715 Maximum hoop force at the encasement (kN/m).

716 Table 9. Settlement (mm) for different area replacement ratios.

717

718 **FIGURE CAPTIONS**

719 Figure 1. 3D finite element model. Reference case.

720 Figure 2. 2D finite element model. Reference case. Circular footing.

721 Figure 3. Mesh sensitivity analyses.

722 Figure 4. Groups of stone columns for different column positions.

723 Figure 5. Influence of column position.

724 Figure 6. Vertical stresses beneath the footing. Diagonal section.

725 Figure 7. Circumferential tensile force of the encasement for different column spacings.

726 Figure 8. Deformation modes: (a) Bulging; (b) Shearing; (c) Punching. Deformed mesh
727 (amplified 10 times). Cross section.

728 Figure 9. Incremental shear strains. Blue (dark) lowest value (0) and red highest value
729 (2%). Cross section.

730 Figure 10. Groups of encased stone columns for different number of columns.

731 Figure 11. Zones at failure: (a) ϕ_s=23º and c_s=3 kPa; (b) ϕ_s=20º and c_s=1 kPa. Black
732 zones: relative shear stress between 99 and 100% of failure.

733 Figure 12. Influence of column length for different column positions.

734 Figure 13. Comparison between small-group and single column. Laboratory tests (Data
735 taken from Ali et al., 2014).

736 Figure 14. Conceptual justification of critical column length in a homogeneous soil
737 layer: (a) for settlement reduction; (b) for bearing capacity.

738 Figure 15. Critical column length for different area replacement ratios and encasement
739 and soil properties. 1 Column (2D) and B=2.5 m: (a) Reference case; (b) c_s= 3
740 kPa and ϕ_s=30º ; (c) J_g=5000 kN/m.

741 Figure 16. Plastic points (in red). Reference case. 1 Column (2D) and B=2.5 m: (a)
742 a_r=10%; (b) a_r=20% ; (c) a_r=50%.

743 Figure 17. Critical partial encasement length for different area replacement ratios and
744 encasement and soil properties. 1 Column (2D) and B=2.5 m: (a) Reference
745 case; (b) c_s= 3 kPa and ϕ_s=30º ; (c) J_g=5000 kN/m.

746

747 Table 1. Column diameter and encasement stiffness for different number of columns.

	a_r=10%	J_g/d_c=1120 kPa	J_g/d_c=2800 kPa
	d_c (m)	J_g (kN/m)	J_g (kN/m)
N=1	1.784	2000	5000
N=4	0.892	1000	2500
N=8	0.631	707.4	1768
N=12	0.515	577.4	1443
N=16	0.446	500.0	1250
N=20	0.399	447.3	1118
N=24	0.364	408.1	1020

748
749
750
751 Table 2. Soft soil and column properties for reference case.

	γ'	K_0	c	ϕ	ψ	ν	E
	(kN/m^3)	(-)	(kPa)	(º)	(º)	(-)	(MPa)
Soft soil	10	0.6	3	23	0	0.33	2
Stone column	10	0.6	0.1	40	5	0.33	30

752

753

754 Table 3. Settlement (mm) for different number of columns.

		J_g/d_c=0		J_g/d_c=1120 kPa		J_g/d_c=2800 kPa	
	L/d_c	Corner	Sides	Corner	Sides	Corner	Sides
2D	5.6	237.6		192.4		164.7	
Circular	5.6	226.9		182.6		156.0	
N=1	5.6	229.5		184.2		156.8	
N=4	11.2	231.4	227.3	176.5	179.3	146.5	150.8
N=8	15.9	231.0	226.8	176.6	177.0	147.9	148.4
N=12	19.4	228.9	226.2	176.6	177.1	147.4	148.5
N=16	22.4	227.3	226.6	176.4	176.7	147.5	148.3
N=20	25.1	226.3	225.2	175.5	176.1	147.1	148.1
N=24	27.5	225.1	224.9	174.4	175.6	146.3	147.7

755 2D, Circular and *N*=1: central column

756

757 Table 4. Maximum hoop force at the encasement, F_g (kN/m), for different number of
758 columns.

	J_g/d_c=1120 kPa		J_g/d_c=2800 kPa	
	Corner	Sides	Corner	Sides
2D	30.4		47.9	
Circular	30.0		47.2	
N=1	31.0		48.2	
N=4	23.3	20.5	35.3	31.5
N=8	18.1	14.7	27.4	22.4
N=12	13.8	11.8	20.9	17.9
N=16	11.5	10.1	17.9	15.6
N=20	10.1	9.1	16.4	14.0
N=24	9.2	8.3	14.4	12.9

759

760

761 Table 5. Normalised maximum hoop force at the encasement, F_g/J_g (%), for different
762 number of columns.

	J_g/d_c=1120 kPa		J_g/d_c=2800 kPa	
	Corner	Sides	Corner	Sides
2D	1.52		0.96	
Circular	1.50		0.94	
N=1	1.55		0.96	
N=4	2.33	2.05	1.41	1.26
N=8	2.46	2.08	1.55	1.27
N=12	2.39	2.04	1.45	1.24
N=16	2.30	2.02	1.43	1.25
N=20	2.26	2.03	1.47	1.25
N=24	2.25	2.03	1.41	1.26

763

764

765 Table 6. Results for different soil material strengths. Reference case.
766
767 (a) Settlement (mm)

	ϕ_s (º)	20	23	26	30
	c_s (kPa)	1	3	6	10
No columns		845.5	291.1	203.9	167.4
2D		291.8	192.4	152.9	135.4
N=1		282.7	184.2	143.2	127.8
N=4	*s*=1 m	275.0	182.0	142.2	127.1
	s=2 m	275.4	181.2	141.3	126.5
	s=3 m	265.2	180.8	140.6	125.2
	s=4 m	253.3	178.7	139.7	123.2

768 2D: central column
769
770 (b) Maximum hoop force at the encasement (kN/m)

	ϕ_s (º)	20	23	26	30
	c_s (kPa)	1	3	6	10
No columns					
2D		46.2	30.4	24.5	23.3
N=1		49.9	31.0	25.2	21.5
N=4	*s*=1 m	26.2	14.8	12.5	11.2
	s=2 m	23.0	14.7	11.8	10.9
	s=3 m	32.4	19.4	14.6	12.9
	s=4 m	36.0	24.6	19.9	16.9

771

772 Table 7. Settlement (mm) for different soil layer thicknesses.

	H/*B*	0.4	0.8	1.2	1.6	2
	H (m)	2	4	6	8	10
No columns		81.0	166.9	236.3	262.6	277.6
2D		47.8	109.3	156.5	181.4	192.4
Circular		45.5	104.3	148.2	171.9	182.6
N=1		46.2	106.4	150.7	174.6	184.2
N=4	*s*=1 m	47.5	106.2	148.7	172.7	182.0
	s=2 m	50.0	107.9	150.3	172.3	181.2
	s=3 m	52.6	110.0	146.4	172.3	180.8
	s=4 m	56.8	110.7	148.4	170.6	178.7

773
774

Table 8. Results for different column lengths. Reference case.

(a) Settlement (mm)

L	2	4	6	8	10
2D	284.0	268.2	238.7	205.6	192.4
Circular	266.5	254.5	225.6	191.6	182.6
N=1	270.3	256.7	226.6	192.2	184.2
N=4	260.5	229.0	196.9	181.8	179.3
N=8	254.6	216.8	185.8	179.1	177.0
N=12	256.4	218.3	186.5	179.3	177.1
N=16	241.2	205.9	180.0	173.7	176.7

Columns on the sides

(b) Maximum hoop force at the encasement (kN/m)

L	2	4	6	8	10
2D	3.3	7.1	19.4	27.1	29.2
Circular	2.4	7.6	19.5	26.2	30.0
N=1	2.5	8.2	20.4	27.6	31.0
N=4	14.8	22.0	21.0	20.4	20.5
N=8	14.2	16.0	14.9	14.6	14.7
N=12	12.3	13.5	12.0	11.8	11.8
N=16	8.7	11.0	9.9	9.6	10.1

Columns on the sides

786 Table 9. Settlement (mm) for different area replacement ratios.

		L=2*B*		*L*=*B*	
		a_r=20%	a_r=30%	a_r=20%	a_r=30%
2D Circular		112.1	86.4	214.8	191.7
N=1		112.4	86.7	214.5	189.8
N=4	*s*=2 m	117.2	86.1	184.6	158.6
	s=3 m	111.3	86.7	167.3	143.3

787

788

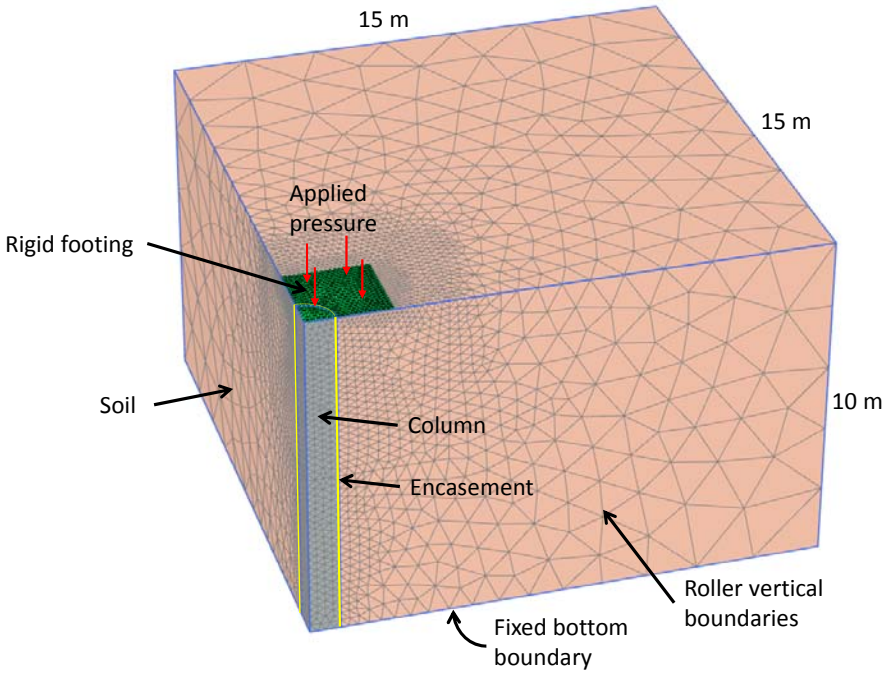

789

790 Figure 1. 3D finite element model. Reference case.

791

792

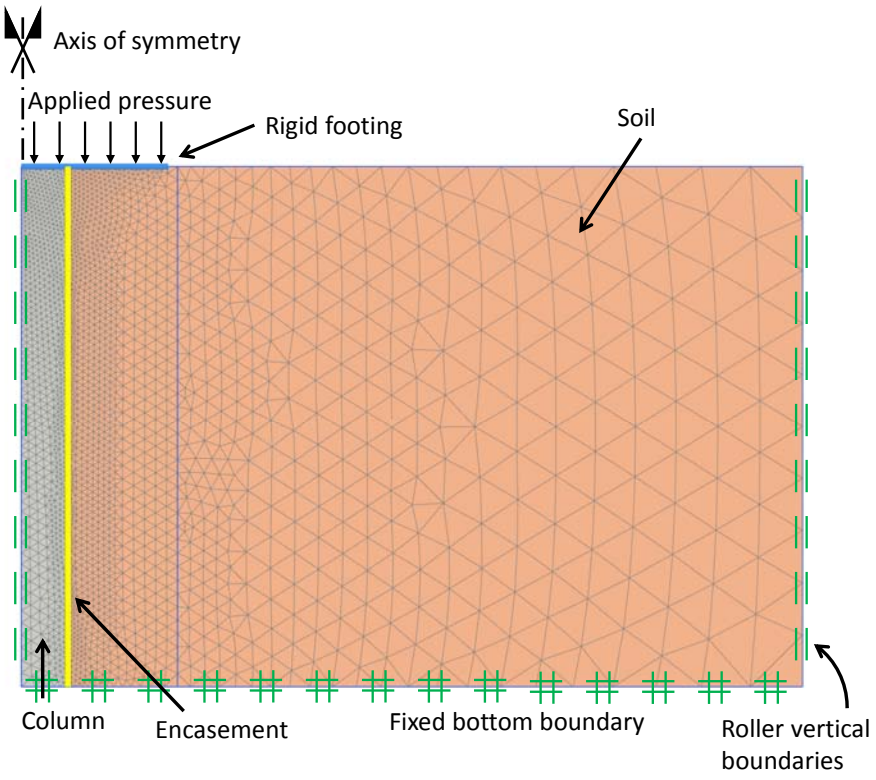

793

794 Figure 2. 2D finite element model. Reference case. Circular footing.

795

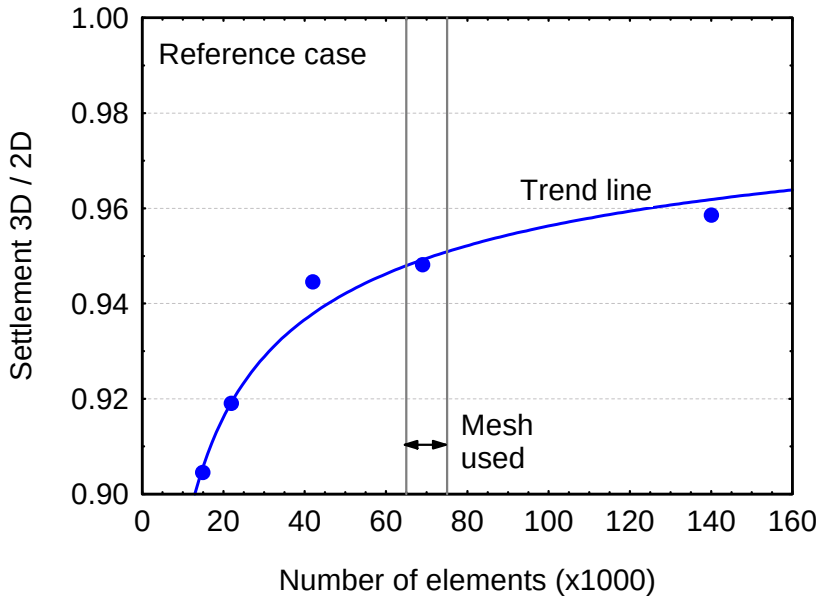

796

797 Figure 3. Mesh sensitivity analyses.

798

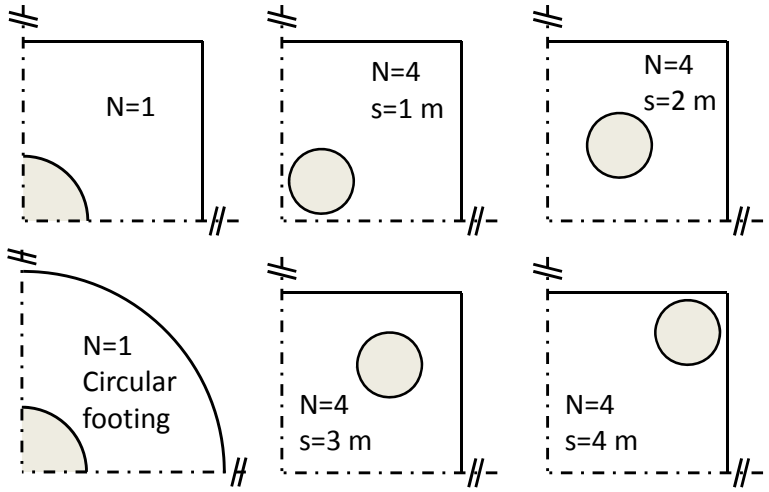

799

800 Figure 4. Groups of encased stone columns for different column positions.

801

802

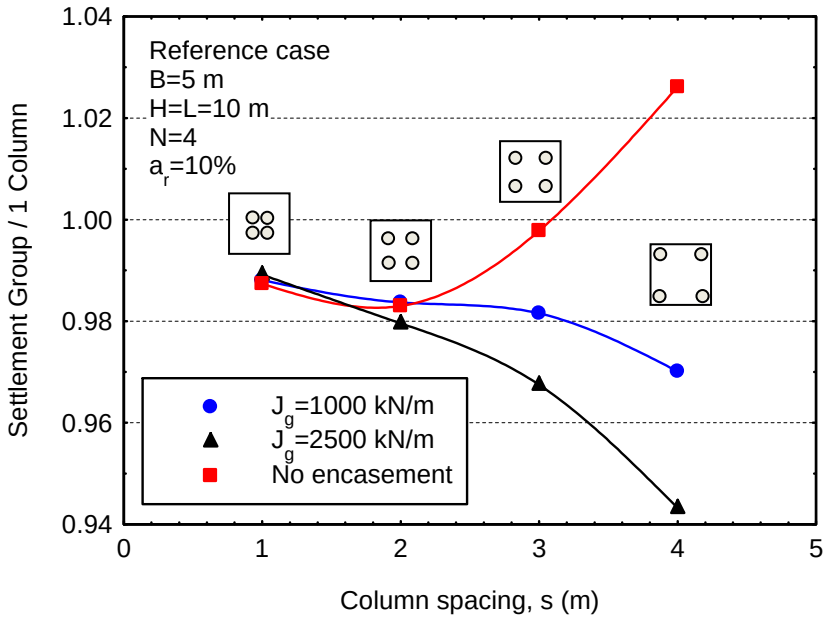

803

804 Figure 5. Influence of column position.

805

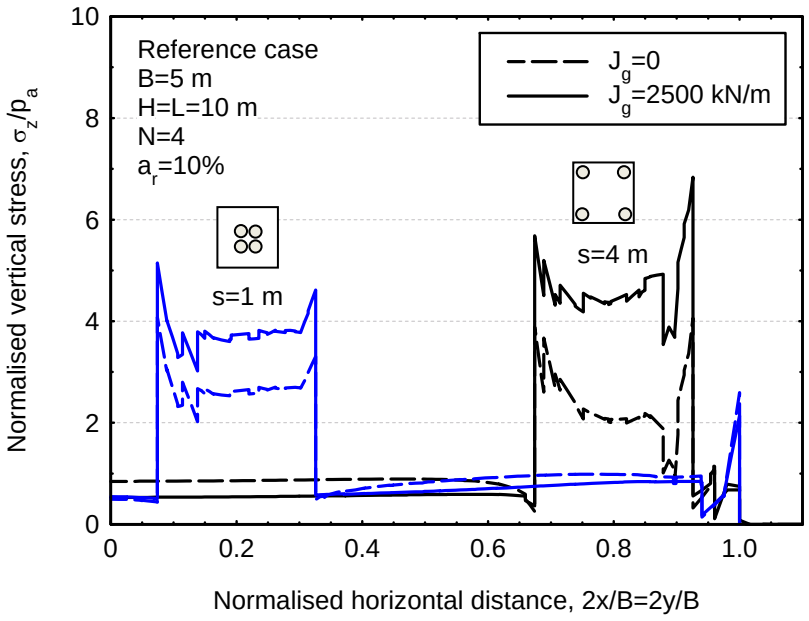

806

807 Figure 6. Vertical stresses beneath the footing. Diagonal section.

808

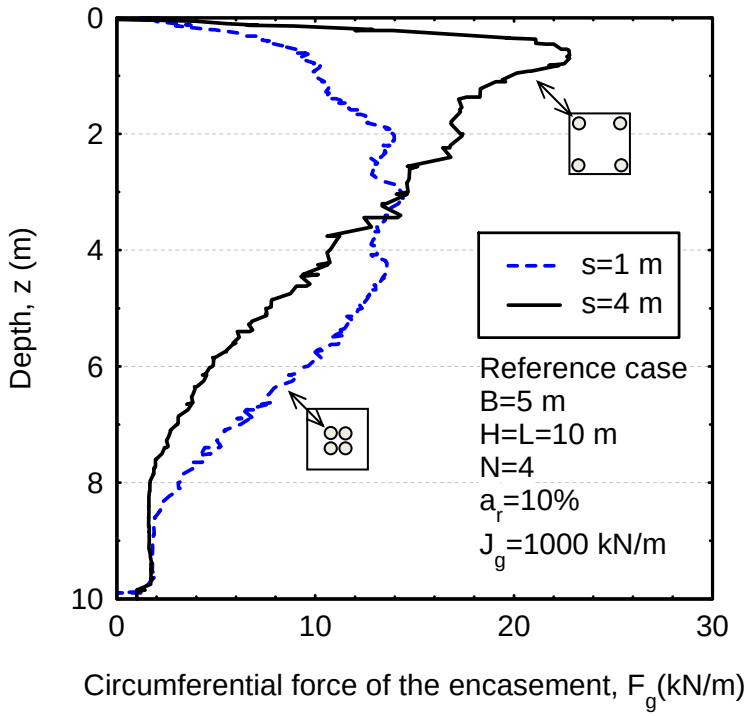

809

810 Figure 7. Circumferential tensile force of the encasement for different column spacings.

811

812

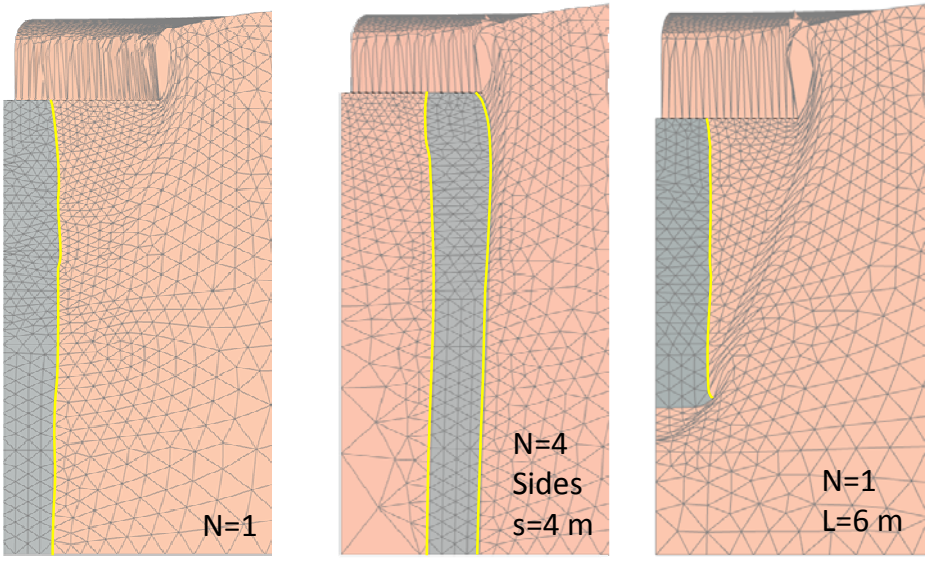

(a) (b) (c)

Figure 8. Deformation modes: (a) Bulging; (b) Shearing; (c) Punching. Deformed mesh (amplified 10 times). Cross section.

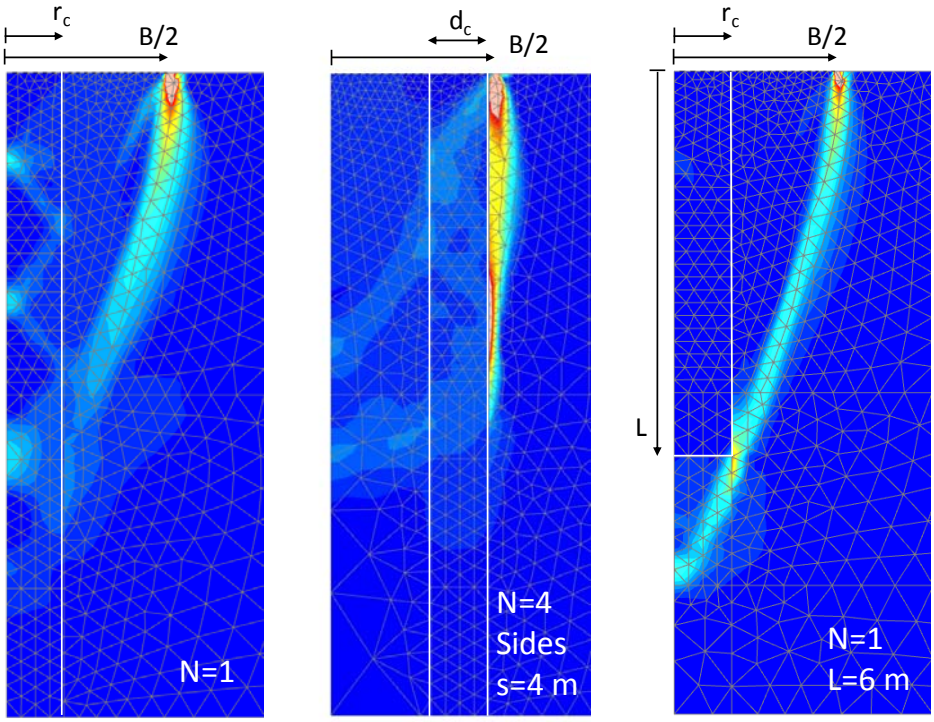

Figure 9. Incremental shear strains. Blue (dark) lowest value (0) and red highest value (2%). Cross section.

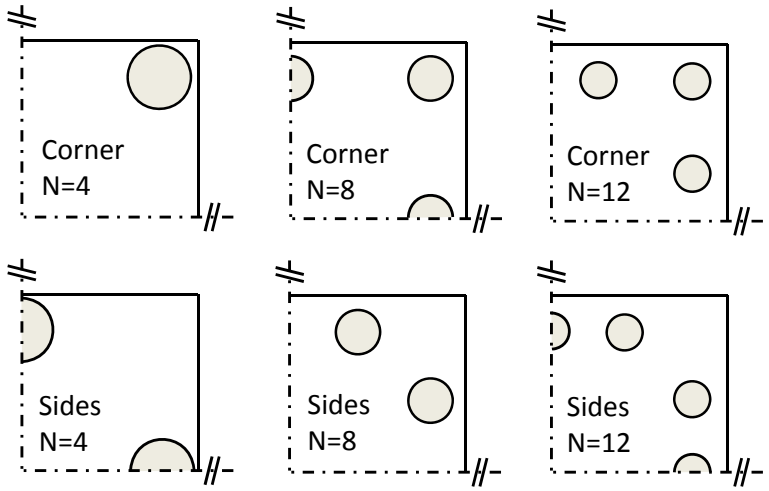

821

822 Figure 10. Groups of encased stone columns for different number of columns.

823

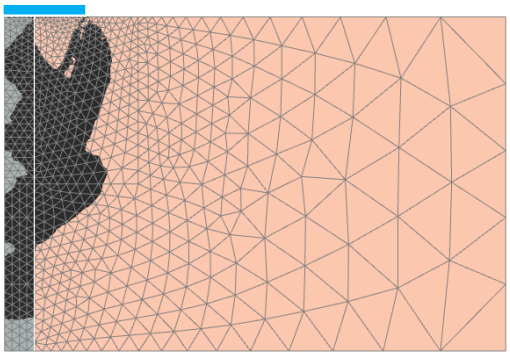

(a)

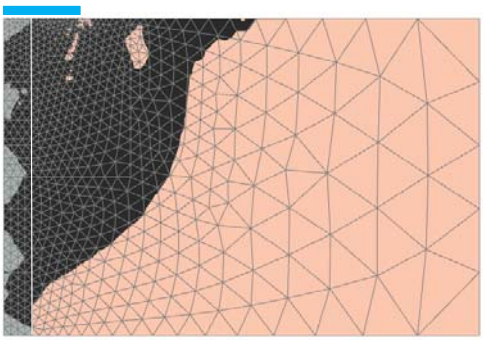

(b)

Figure 11. Zones at failure: (a) ϕ_s=23º and c_s=3 kPa; (b) ϕ_s=20º and c_s=1 kPa. Black area: relative shear stress between 99 and 100% of failure.

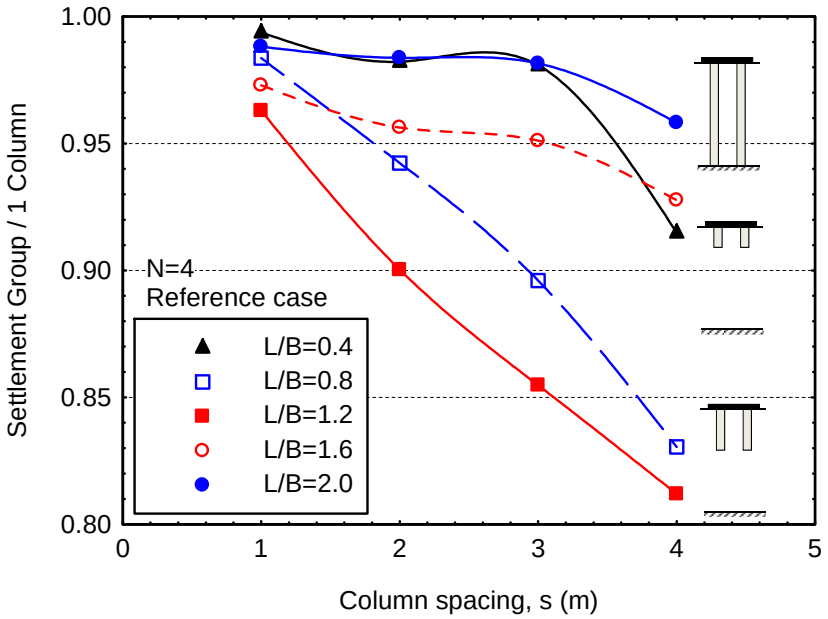

832

833 Figure 12. Influence of column length for different column positions.

834

835

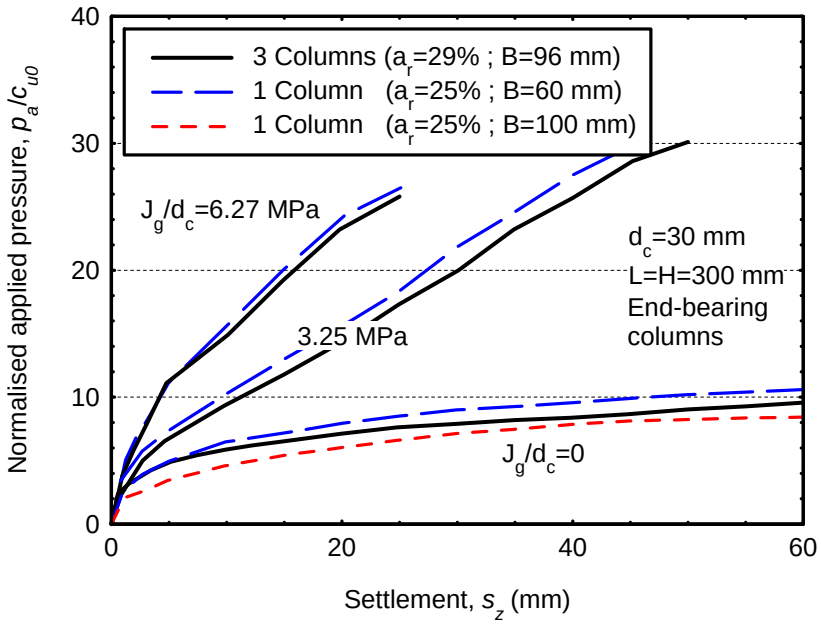

836

837 Figure 13. Comparison between small-group and single column. Laboratory tests (Data taken from Ali et

838 al., 2014).

839

840

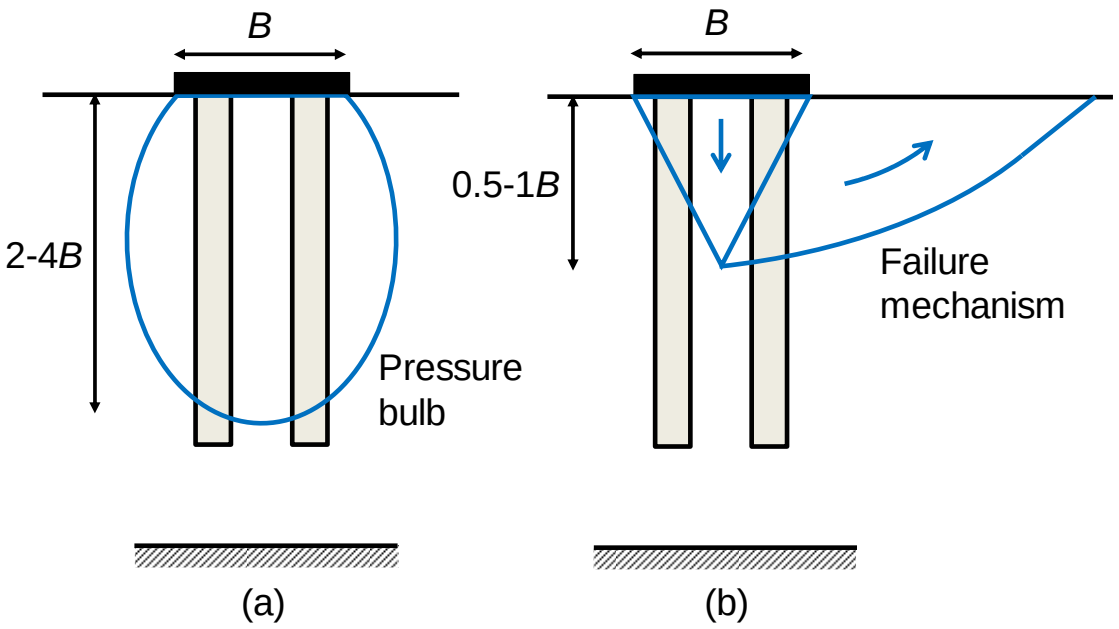

841

842 Figure 14. Conceptual justification of critical column length in a homogeneous soil layer: (a) for
843 settlement reduction; (b) for bearing capacity.

844

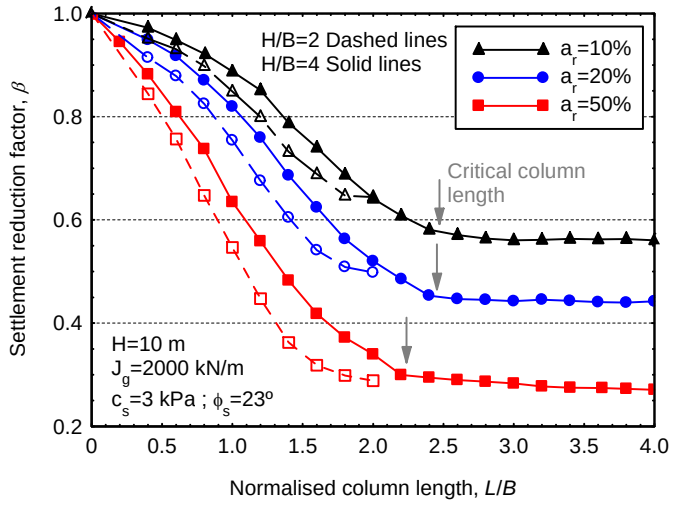

845 (a)

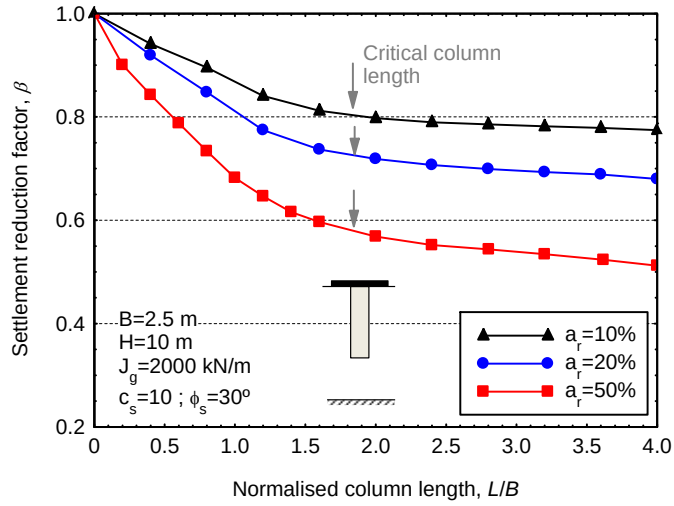

846 (b)

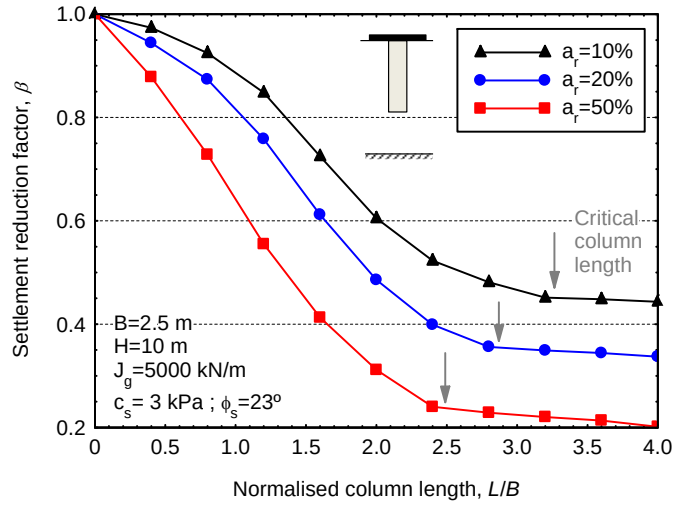

847 (c)

848 Figure 15. Critical column length for different area replacement ratios and encasement and soil properties.

849 1 Column (2D) and B=2.5 m: (a) Reference case; (b) c_s= 3 kPa and ϕ_s=30º ; (c) J_g=5000 kN/m.

850

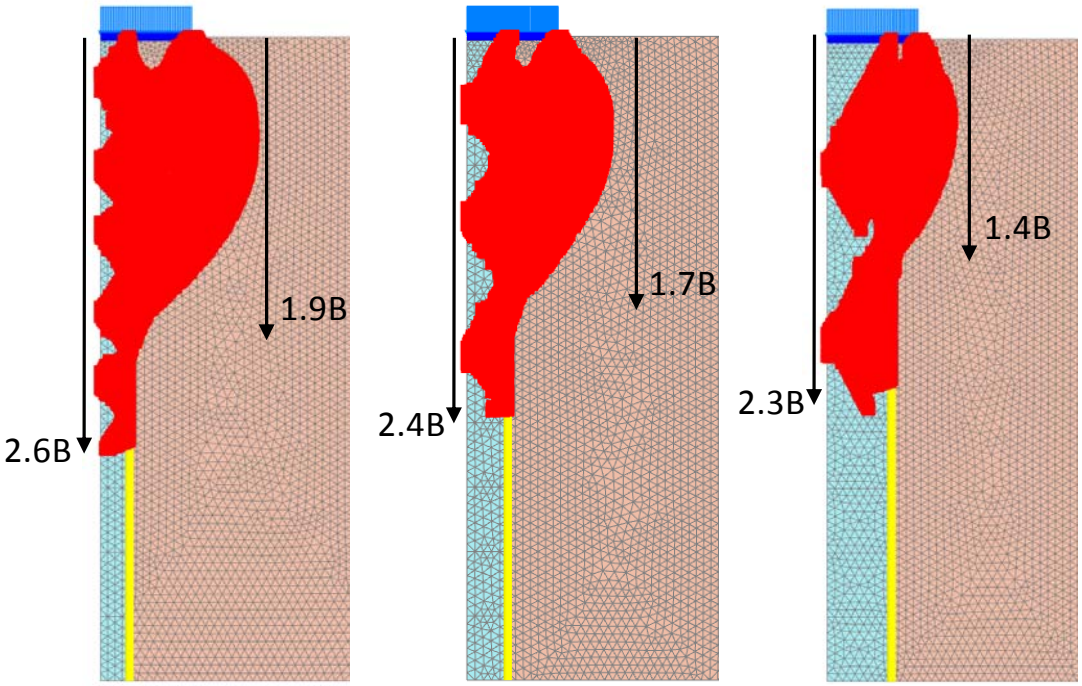

Figure 16. Plastic points (in red). Reference case. 1 Column (2D) and B=2.5 m: (a) a_r=10%; (b) a_r=20% ; (c) a_r=50%.

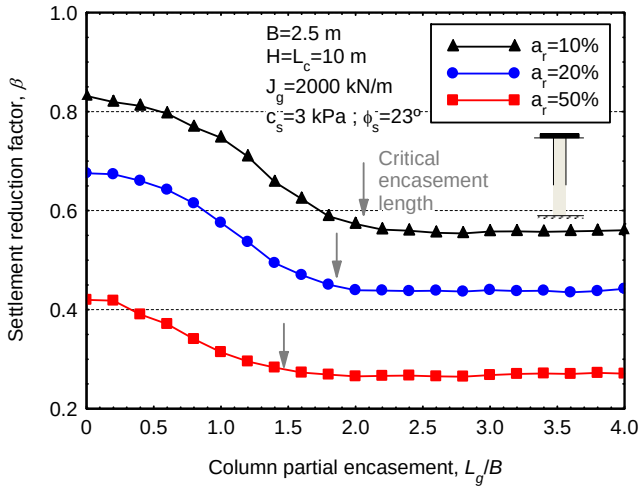

856 (a)

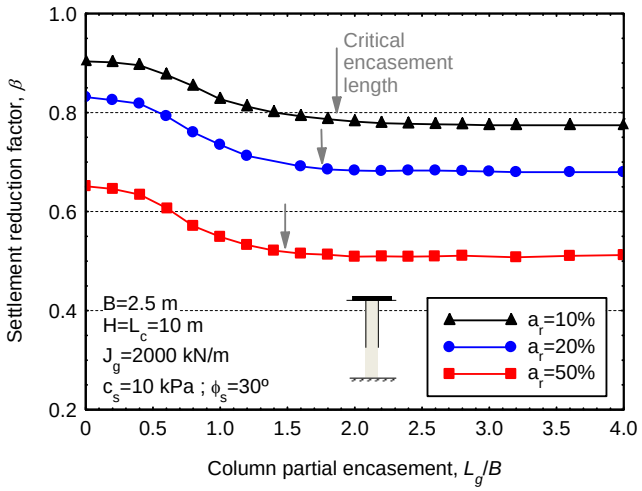

857 (b)

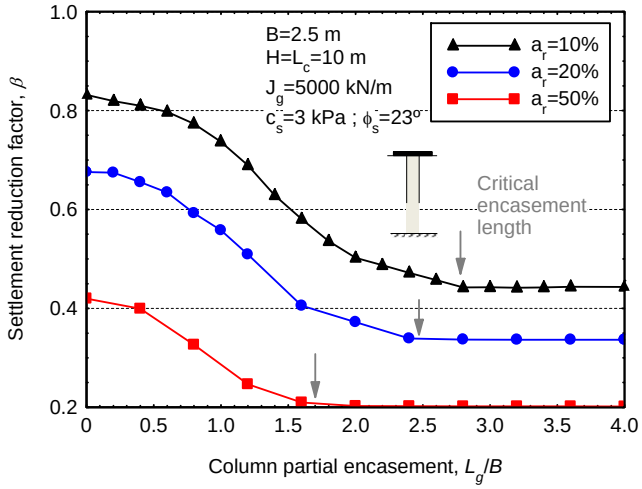

858 (c)

859 Figure 17. Critical partial encasement length for different area replacement ratios and encasement and soil
860 properties. 1 Column (2D) and B=2.5 m: (a) Reference case; (b) c_s= 3 kPa and ϕ_s=30º ; (c) J_g=5000 kN/m.